Hindawi
Mathematical Problems in Engineering
Volume 2022, Article ID 1864290, 12 pages
https://doi.org/10.1155/2022/1864290

*Research Article*

# Cooperative Communications Based on Deep Learning Using a Recurrent Neural Network in Wireless Communication Networks

**M. Rathika,[1] P. Sivakumar,[2] K. Ramash Kumar,[3] and Ilhan Garip[4]**

[1]*Department of Electronics and Communication Engineering, Kingston Engineering College, Vellore, Tamil Nadu, India*
[2]*Department of Electronics and Communication Engineering, Dr. N. G. P Institute of Technology, Coimbatore, Tamil Nadu, India*
[3]*Department of Electrical and Electronics Engineering, Dr. N. G. P. Institute of Technology, Coimbatore 48, Tamil Nadu, India*
[4]*Department of Electrical and Electronics Engineering, Nisantasi University, Istanbul, Turkey*

Correspondence should be addressed to K. Ramash Kumar; ramashkumar@drngpit.ac.in

Received 14 September 2022; Revised 30 November 2022; Accepted 13 December 2022; Published 21 December 2022

Academic Editor: Jun Li



In recent years, cooperative communication (CC) technology has emerged as a hotspot for testing wireless communication networks (WCNs), and it will play an important role in the spectrum utilization of future wireless communication systems. Instead of running node transmissions at full capacity, this design will distribute available paths across multiple relay nodes to increase the overall throughput. The modeling WCNs coordination processes, as a recurrent mechanism and recommending a deep learning-based transfer choice, propose a recurrent neural network (RNN) process-based relay selection in this research article. This network is trained according to the joint receiver and transmitter outage likelihood and shared knowledge, and without the use of a model or prior data, the best relay is picked from a set of relay nodes. In this study, we make use of the RNN to do superdimensional (high-layered) processing and increase the rate of learning and also have a neural network (NN) selection testing to study the communication device, find out whether or not it can be used, find out how much the system is capable of, and look at how much energy the network needs. In these simulations, it has been shown that the RNN scheme is more effective on these targets and allows the design to keep converged over a longer period of time. We will compare the accuracy and efficiency of our RNN processed-based relay selection methods with long short-term memory (LSTM), gated recurrent units (GRU), and bidirectional long short-term memory (BLSTM),which are all acronyms for long short-term memory methods.

## 1. Introduction

Along with several applications, wireless communication methods have some disadvantages. Wireless signals are easily hacked, which compromises privacy. In wireless networks, security algorithms (AES, WEP, and WAP2) and modulation techniques (FHSS and DSSS) are used to avoid this. Wireless networks were slower in the past. Wireless LANs with advanced standards like IEEE 802.11ac and 802.11ad are now available, providing performance comparable to classic Ethernet-based LANs. At the outset of a wireless network's implementation, meticulous radio frequency planning is required. Interference is a problem with wireless communication. There are a variety of receiver and modulation techniques that can make a wireless system resistant to interference. Despite the fact that 4G networks are the greatest for mobile consumers, they do have some drawbacks. One of the most significant issues is the operational area, which is a disadvantage of all communication networks, including 2G and 3G. In today's modern world, many rural locations and many buildings in large centers are without network service.

This is due to our current communication standards and equipment, which should be updated for this latest technology, which has the potential to bring communication and many other has advanced applications everywhere, but only if our operational area is effectively enhanced. One of the most significant obstacles to delivering large data rates while maintaining the requisite quality of service is the unreliability of the wireless medium, which is caused by inherent channel fading. Furthermore, because high frequency bands are being employed for future wireless generations, transmission losses grow considerably with distance travelled. As a result, 3G and 4G long-term evolution (LTE) standards encourage denser deployment of base stations in conjunction with enhanced multiantenna systems in order to ensure that links are stable and that extreme spectral efficiency criteria are met. The topic of relay selection has received a lot of attention [1, 2].

Most solutions concentrate on the various selection of relay nodes or users which connect to selected relays or whether mobile or host fixed system, which are generally specialized devices for specific network characteristics. From 2019, most of the cellular companies started deploying 5G technology standard for the broadband cellular networks. There is a transformation in the 5G networks regarding their speed, latency, and connectivity with the huge number of devices especially in the areas of IoT, VR, and artificial intelligence (AI). Several researchers offer AI-based solutions, especially deep learning (DL), due to their capacity to adapt to dynamic conditions, such as wireless network mobility; these approaches enable the efficient solution of challenging challenges [3]. In networking, machine learning is used to solve a variety of issues, including routing [4]. We have chosen to concentrate on the relay selection process.

## 2. Cooperative Communications

As previously stated, cooperative communications (CC) contribute to increased system dependability. Cooperative diversity is a type of spatial diversity [5]. Some common cooperative methods are amplify and forward [3, 4, 6], as well as decode and forward. The relays receive the information, amplify the signal, and then send it to the destination in the first method, while in the second approach, the relays completely decode the original signal, re-encode it, and then send it to the destination. Because in addition to relays' deliver, these are the original signal approaches that are known as redundancy-based agreeable calculations. The nodes are needed distinct inside the channels limited bandwidth. Distributive space time coding (DSTC) [7] is a technique that can be applied to achieve diversity in collaboration and avoid bandwidth constraints. The DSTBC is a distributed system variant of STBC's, as described in reference [8], in which a duplicate of the data is shared across participating transmitting nodes. We assume a system with only one relay and stress these techniques because currently, we are working with DSTBC and cooperative diversity that are two terms that come to mind while thinking about DSTBC. To make things easier, relay selection was recommended construction of cooperative networks, motivated by the advantage of selection variety from multiuser selection and antenna selection. The authors of reference [9] proposed a location-based technique for selecting the best relay based on geographical random forwarding notions [10]. Assuming that each node is aware of both its own and the destination's position, the relay is the node closest to the destination. Because determining positions or distances between all nodes is not a straightforward task, such algorithms are better suited for static networks but less so for mobile networks.

Opportunistic relay selection (ORS) [11], on the other hand, is a single-relay strategy that does not need topological knowledge. This approach selects a single relay with the best channel condition based on local channel measurements (in accordance to a given selection criterion [12]. When compared to more complicated protocols such as DSTC, ORS has no performance penalty in terms of the multiplexing-diversity tradeoff. Most importantly, it decreases implementation complexity by obviating the requirement for space-time codes and avoids synchronization among several transmitting relays. It was discovered to be a simple yet efficient way to achieve cooperative diversity in slow fading channels. However, in a quickly fading wireless environment, the measured channel state information (CSI) for relay selection may differ from the actual channel quality at the time of signal relaying due to processing and feedback delays. As frequently demonstrated in [13–17], obsolete CSI results in incorrect relay selection, which significantly degrades ORS performance.

The problem of obsolete CSI will worsen as high-mobility applications proliferate and higher frequency bands are adopted in 5G and beyond systems. Sending signals at higher frequencies (such as millimeter wave and terahertz communications) or moving at a faster speed (e.g., vehicular communications, high-speed trains, and unmanned aerial vehicles) will increase the frequency shift, resulting in a faster time-varying channel, according to the Doppler effect in signal propagation. As a result, for next-generation wireless communications, the development of a simple cooperative approach that can also be used to rapidly fading channels is becoming increasingly critical [17–20].

## 3. Literature Review

The issues that have emerged in the helpful correspondence organization since the proposed helpful correspondence plot are how to get transfers to join participation and select transfers to help others. As the correspondence hubs are not helpful essentially, impetus is expected to urge hubs to take part in the agreeable correspondence networks as sending hubs. In a work by Mishra et al. [4], evaluation is acquainted with an urge for the transfer hubs to join the collaboration and to match viable application. Hand-off hubs are given motivating forces in a type of installment for utilization of the asset they spent on sending the data for different hubs. Many works have been done in the field of transfer choice for agreeable correspondence organizations. In reference [21], the creator proposed a hand-off choice in light of the area of the transfer hubs. Hand-off determination in light of momentary connection with obstruction is done in reference [22].

Disseminated hand-off determination utilizing game hypothesis [23] centers around the limit of the absolute transmission. After the transfer choice, the asset distribution and improvement is a following issue in the helpful correspondence organization. Assigning ideal asset to each hand-off hub with various goals between the hubs in the framework is expected to acquire best execution from the agreeable correspondence organization. An agreeable correspondence network with both transfer hubs and source hub needs to expand their own benefit through asset designation, and enhancement will have different asset distributions and streamlining processes than where the goal is just to boost the source hub gain. Most algorithms, as we will see in this section, focus on the selection of dedicated relays or assume that some information is available a priori to facilitate the selection process. The first portion of section 2 will address traditional methods, while the second part will provide machine learning algorithms. Classical algorithms are approaches for solving problems that do not use machine learning. Using matching theory [21, 22], Markov chains [22, 23], or framing the topic as a maximization problem [24] are some examples. The matching game is used by the authors of reference [21] to estimate future radio circumstances for flying drones.

The position and trajectory of the drones are used to dynamically change each one's transmission mode and decide which drones will deliver data. However, in the context of transportation, it is not always viable to predict users' future paths. The authors of reference [22] suggest a relay selection method in which mobile users (MU) pick relays based on cost. The model is made up of a base station, numerous relays, and several MUs. A transition matrix represents user mobility, and a restricted Markov decision process is used to simulate the problem. Despite the fact that user mobility is taken into consideration in this proposal, the usage of dedicated relays limits the problem.

The approach presented in reference [24] seeks to optimize the system throughput while fulfilling user QoS requirements while taking into account a power limitation. The model consists of a single antenna, multiple fixed relays, and users. The maximizing problem enables the selection of the best relay for each user. However, because relays are fixed units with no mobility, the approach is ineffective in a highly dynamic environment with possible relays moving in and out of the investigated region.

The authors of reference [23] recommend that multirelay selection (MRs) be included to assist manage heavy traffic times of stationary relays in order to decrease signaling overhead and improve user mobility experience. Markov chains are used to represent high traffic times. Despite their mobility, MRs are designed to be installed on vehicles such as buses and move at a steady speed. This may not be appropriate in low-population-density areas. The authors of reference [25] suggest a relay selection technique to help nodes with heavy interference. A macro cell antenna, a few pico cell antennas, and many users comprise the model. This method is intriguing since each node has the capacity to transmit data to assist another node. However, it employs static nodes and is not suited for usage in a highly mobile environment.

In the literature, many virtual-multiple input multiple output (V-MIMO) designs have been proposed to achieve spatial variety [3, 4], spatial multiplexing [21], and/or beam forming [22].The amplify-and-forward [22], decode-and-forward [23], and compress-and- forward [24] protocols have been used to achieve two-hop [23] or multi-hop [25] communication from a relay viewpoint. Furthermore, V-MIMO may be investigated at the link or system level [22]. In addition, ergodic capacity [22], outage capacity, bit error rate (BER), and energy efficiency have all been used to evaluate performance of V-MIMO. The selection of relay users is another key element that has a direct impact on V-MIMO performance. Several techniques for cooperative relay selection have been presented. Some of the major work is provided in reference [7], where the user pairing method based on orthogonally of the channel matrix is explored, and group-based user pairing is proposed in reference [9].

Wireless communication and networks (WCNs) is a network where a group of N number of devices can transmit and receive the data over radio frequencies without the usage of any physical connections like wires or cable. The key parameters of wireless communication and networking are signal encoding and decoding techniques, spectrum limit, error detection and correction techniques, and architecture of the network. WCNs plays a major role in telecommunications and networking such as usage of cellular networks, wireless LANs, and different kinds of satellite services [5, 9].

## 4. System Model

This section initially covers the basics of deep recurrent networks, such as the simple recurrent neural network (RNN), long short-term memory (LSTM) [26], and gated recurrent unit (GRU) [27], before going into how to use one to develop a channel predictor [28, 29]. The computational complexity and statistics of projected CSI are also examined for these predictors [30–32]. Unlike feed-forward neural networks, which have unidirectional input flow, RNNs include recurrent self-connections that allow them to memories previous data and show a significant promise in time-series prediction [33]. The previous time step's activation is transmitted back as part of the current step's input. The $l^{th}$ recurrent layer of a basic RNN is usually described as follows:

$$d_t^{(l+1)} = R^{(l)}\left(d_t^{(l)}\right) = \delta_h\left(W^{(l)} d_t^{(l)} + U^{(l)} d_{t-1}^{(l+1)} + b^{(l)}\right), \tag{1}$$

where $W^{(l)}$ and $U^{(l)}$ in equation (1) are matrices of weights for the $l^{th}$ layer, $b^l$ is a vector of bias, $d_t^{(l)}$ and $d_{t-1}^{(l+1)}$ represent the input and output for layer 1 and $(1+1)$, respectively, *and* $d_{t-1}^{(l+1)}$ is the result of the previous step's feedback, $R^{(l)}$ [34]. The activation function frequently picks the hyperbolic tangent indicated by and is the relation for the input and output of the $l^{th}$ RNN hidden layer, tan $h$, *i.e.*, $\delta_h(x) = (e^{2x} - 1)/(e^{2x} + 1)$.

Utilizing average stochastic-inclination drop (SGD) strategy to prepare a repetitive organization, the back-spread blunder signals will generally zero that suggests a restrictively lengthy intermingling time [35–40]. To handle this inclination disappearing issue, Hochreiter and Schmidhuber proposed long short-term memory (LSTM) in their trailblazer work of reference [26], which brought cell and entryway into the RNN structure. The previous is a unique memory unit and the last option controls read

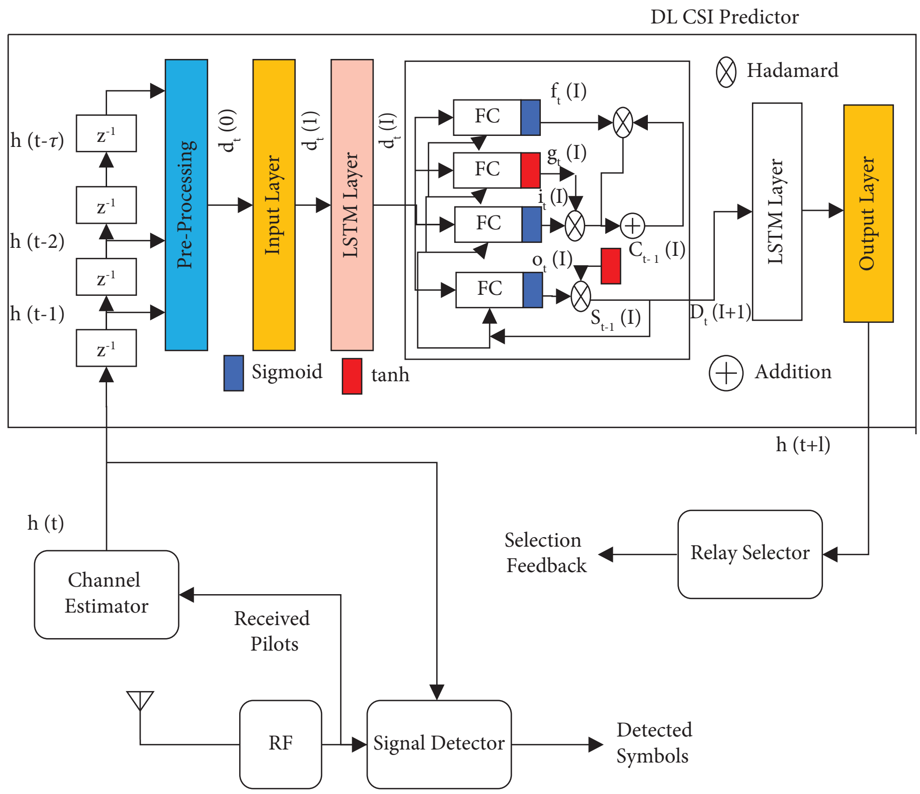


FIGURE 1: Graphical block diagram representation of the receiver [29].

and compose admittance to the cell. In 1999, Jiang et al. [41] further presented another entryway that figures out how to reset the secret state at fitting times. Then, at that point, a typical LSTM cell has three entryways: an information door controlling the degree of new data streams into the cell, a neglect door to sift through futile memory, and a result entryway that controls the degree to which the memory is applied to create the initiation. The upper piece of Figure 1 shows the graphical portrayal of a profound LSTM network comprising of an information layer, $L$ secret layers, and a result layer. How about we utilize the $l^{th}$ stowed away layer as an illustration to reveal insights into how an initiation signal goes through the organization? There are two secret states—the present moment $S_{t-1}^{(l)}$ and the long-term state $C_{t-1}^{(l)}$; the input $d_t^{(l)}$ and $S_{t-1}^{(l)}$ the activation vectors for the gates are generated by combining the activation vectors of four fully connected (FC) layers [29, 33].

$$\begin{aligned} i_t^{(l)} &= \delta_g\left(W_i^{(l)} d_t^{(l)} + U_i^{(l)} S_{t-1}^{(l)} + b_i^{(l)}\right), \\ o_t^{(l)} &= \delta_g\left(W_o^{(l)} d_t^{(l)} + U_o^{(l)} S_{t-1}^{(l)} + b_o^{(l)}\right), \\ f_t^{(l)} &= \delta_g\left(W_f^{(l)} d_t^{(l)} + U_f^{(l)} S_{t-1}^{(l)} + b_f^{(l)}\right), \end{aligned} \quad (2)$$

where $W$ and $U$ are weight matrices for the FC layers, $b$ stands for bias, and the subscripts $i$, $o$, and $f$ stand for input, output, and forget gate, respectively, and $\delta_g$ is an abbreviation for the logistic sigmoid function, $\delta_g(x) = (1/(1+e^{-x}))$. The current long-term state $c_t^{(l)}$. is obtained by first erasing old memory using the forget gate, then by adding fresh data picked by the input gate [42], $c_t^{(l)} = f_t^{(l)} \otimes c_{t-1}^{(l)} + i_t^{(l)} \otimes g_t^{(l)}$, where the Hadamard product (element-wise multiplication) is denoted by the operator $\otimes$ and $g_t^{(l)} = \delta_g(W_g^{(l)} d_t^{(l)} + U_g^{(l)} S_{t-1}^{(l)} + b_g^{(l)})$. This hidden layer's output is calculated by the following expression:

$$d_t^{(l+1)} = L^{(l)}\left(d_t^{(l)}\right) = o_t^{(l)} \otimes \delta_h\left(c_t^{(l)}\right), \quad (3)$$

where $L^{(l)}$ represents the LSTM's $l^{\text{th}}$ layer's input-output function. It is worth noting that the output is the present short-term condition, i.e., $S_t^{(l)} = d_t^{(l+1)}$ [29].

Figure 1 shows a block diagram of the receiver, which includes an input layer, an output layer, and $L$ hidden layers, as well as a DL-based channel predictor [29]. The $l^{th}$ hidden layer is opened to detail the internal structure of an LSTM memory block and its information flow. To maintain authentic channel data, a tapped-postpone line is applied to shape a progression of back to back CSI tests for the information layer [26, 43, 44]. The indicator is embedded between the channel assessor and hand-off selector, changing estimated CSI to anticipated CSI straightforwardly with practically no different adjustments for an ORS framework. LSTM has acquired huge accomplishment notwithstanding its concise history and has been financially executed in different AI items like Apple Siri and Google Translate. Following its presentation, mainstream researchers created various varieties, the most notable of which was GRU presented by Cho et al. in reference [27]. It is a less complex adaptation with fewer boundaries; yet, it outflanks LSTM on some more modest and less continuous

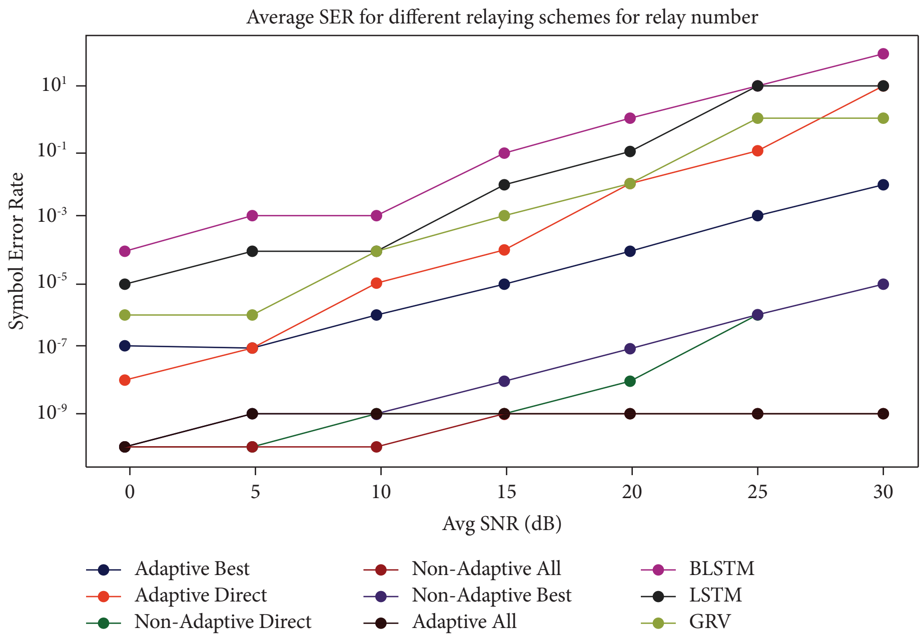


FIGURE 2: Average SER for different relaying schemes for relay number 3 (R3).

datasets. To improve on the design, a GRU memory cell has just a solitary secret state, and the quantity of entryways is diminished to two: the update and reset door. The activation vector for the update gate is computed by $d_t^{(l)} = \sigma_g (W_z^{(l)} d_t^{(l)} + U_z^{(l)} S_{t-1}^{(l)} + b_z^{(l)})$, which decides the extent to which the memory content from the previous state will remain in the current state. The reset gate controls whether the previous state is ignored, and when it tends to 0, the hidden state is reset with the current input. It is given by by $d_t^{(l)} = \sigma_g (W_r^{(l)} d_t^{(l)} + U_r^{(l)} S_{t-1}^{(l)} + b_r^{(l)})$. The previous concealed state was the same way, $S_{t-1}^{(l)}$ runs through the cell, deletes old memory, and replaces it with fresh material, resulting in the current concealed state.

$$s_t^{(l)} = \left(1 - z_t^{(l)} \otimes S_{t-1}^{(l)} + z_t^{(l)} \otimes \sigma_h\left(W_s^{(l)} d_t^{(l)} + U_s^{(l)}\left(r_t^{(l)} \otimes S_{t-1}^{(l)}\right) + b_s^{(l)}\right)\right). \quad (4)$$

The hidden state is also equal to its output of this hidden layer, i.e. $d_t^{(l+1)} = G^{(l)} (d_t^{(l)}) = s_t^{(l)}$, where $G^{(l)} (.)$ denotes the input-output function.

## 5. Simulation Results

In this segment, the analysis of CC techniques such as all relay participation-based DF techniques and BRS- based DF technique under perfect CSI has been considered. The performance characteristics such as the SNR, SER, PA factor, and BER of the all relay participation technique and BRSS have been evaluated [45]. The SNR, SER, PA factor, and BER of the cooperative techniques have been evaluated. The parameters desired for the analysis are target BER = 0.0001 and the SNR range is from 0 to 30 dB.

In Figure 2, the SER comparison characteristic curves for all RP-DF schemes, best RP-DF schemes and direct communication scheme under adaptive and non-adaptive

TABLE 1: Average SER for different relaying schemes for relay number 3 (R3).

| Scheme | SER | | | | | | |
|---|---|---|---|---|---|---|---|
| BLSTM | $10^{-4}$ | $10^{-3}$ | $10^{-3}$ | $10^{-1}$ | $10^{0}$ | $10^{1}$ | $10^{2}$ |
| LSTM | $10^{-5}$ | $10^{-4}$ | $10^{-4}$ | $10^{-2}$ | $10^{-1}$ | $10^{1}$ | $10^{1}$ |
| GRV | $10^{-6}$ | $10^{-6}$ | $10^{-4}$ | $10^{-3}$ | $10^{-2}$ | $10^{0}$ | $10^{0}$ |
| Adaptive best | $10^{-7}$ | $10^{-7}$ | $10^{-6}$ | $10^{-5}$ | $10^{-4}$ | $10^{-3}$ | $10^{-2}$ |
| Adaptive direct | $10^{-8}$ | $10^{-7}$ | $10^{-5}$ | $10^{-4}$ | $10^{-2}$ | $10^{-1}$ | $10^{1}$ |
| Non-adaptive direct | $10^{-10}$ | $10^{-10}$ | $10^{-9}$ | $10^{-9}$ | $10^{-9}$ | $10^{-6}$ | $10^{-5}$ |
| Non-adaptive all | $10^{-10}$ | $10^{-10}$ | $10^{-10}$ | $10^{-9}$ | $10^{-9}$ | $10^{-9}$ | $10^{-9}$ |
| Non-adaptive best | $10^{-10}$ | $10^{-9}$ | $10^{-9}$ | $10^{-8}$ | $10^{-7}$ | $10^{-6}$ | $10^{-5}$ |
| Adaptive all | $10^{-10}$ | $10^{-9}$ | $10^{-9}$ | $10^{-9}$ | $10^{-9}$ | $10^{-9}$ | $10^{-9}$ |

scenarios have been designed as a function of average SNR, when the relay number is fixed as 3 [46]. From these curves, it can be observed that all adaptive schemes outperform the nonadaptive schemes. It can be noted that the direct transmission provides the greatest average SER compared to the other two schemes and the SER decreases as the SNR increases. The mathematical values of SER comparison are mentioned in Table 1. It is also observed that the BRSS outperforms the all relay participation scheme by 2 bits/s at low SNR and 6 bits/s at high SNR [47]. Figure 3 shows the best correlation of various relay system mechanism and BLSTM integrated relay mechanism. Here, the heatmap is provided with 2-dimensional with correlation between the variables on each axis is mentioned by each square. The range of correlation is generally between −1 and +1. There is a no linear relationship between the variables when the value is closer to zero and when it is closer to 1, and then, we can consider it as highly positive correlated. The dark purple color denotes that there is high correlation and the light blue color indicates that correlation is less between the given variables.

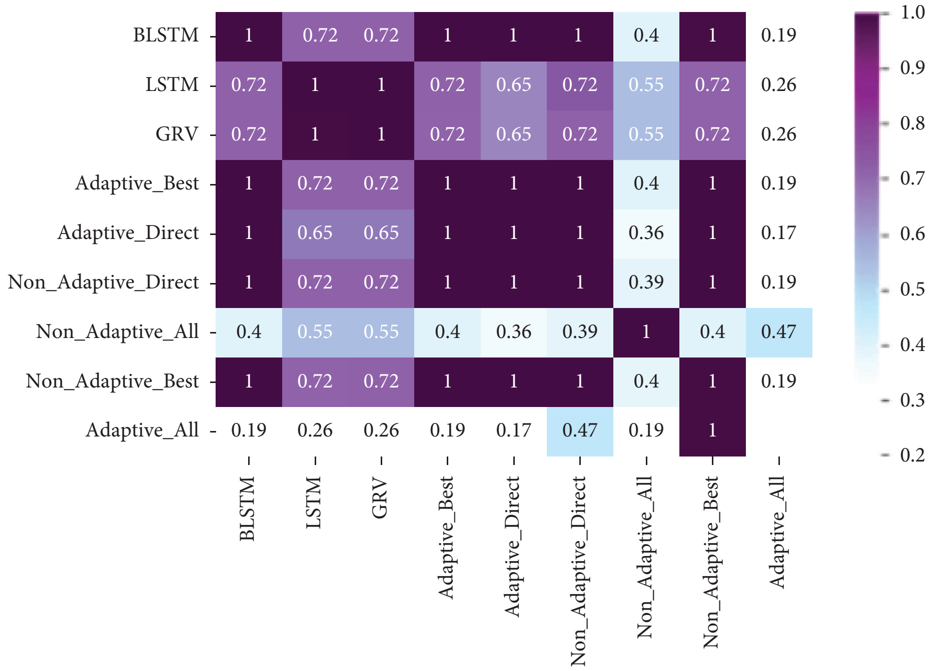


Figure 3: Heatmap co-variance relation for average SER for different relaying schemes for relay number 3 (R3).

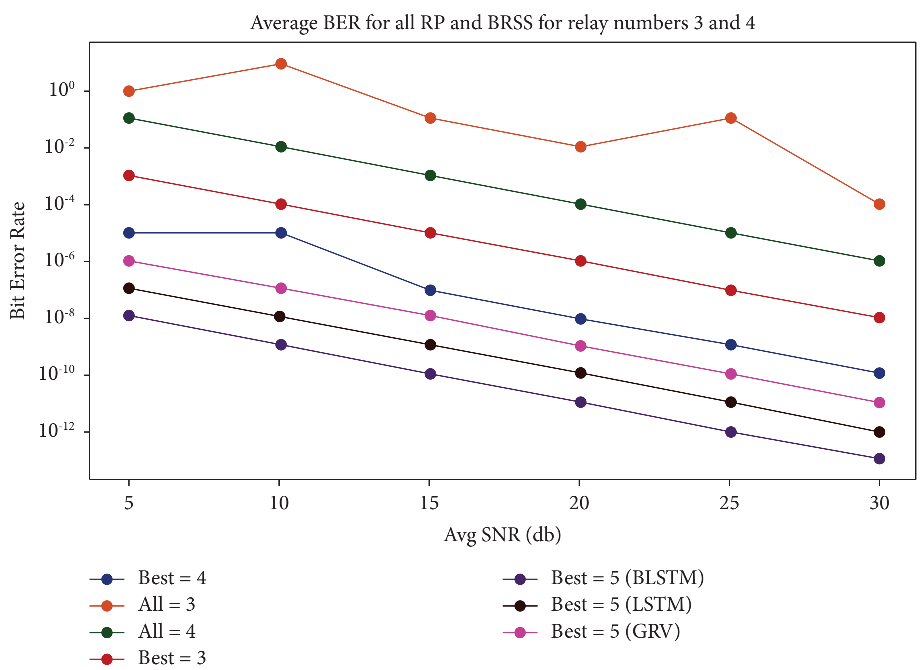


Figure 4: Average BER for all RP and BRSS for relay numbers 3 and 4 (R4).

Figure 4 displays the average BER characteristic curves of entire RP and BRSS for relay numbers 3 and 4. From these plots, it can be viewed that the BER of adaptive BRS is below the target BER [48]. Table 2 provides the average BER values from Figure 4. When the channel state is poor, that is, when the average SNR is low, the BER is excessive and average SNR increases the BER decreases. The value of BER also decreases as the no. of relay increases. The BER of BRS is 0.0001 lower compared to the all relay participation schemes at 30 dB [49]. Figure 5 shows the relation of various relay system mechanism and BLSTM integrated relay mechanism shows the best correlation with all the relaying schemes.

Figure 6 and Table 3 show the PA characteristic plots and values, respectively, of all the adaptive and non-adaptive schemes such as all relay participation schemes, BRSS, and direct communication scheme for varying relay numbers. From these plots, it has been verified that all adaptive schemes outperform the non-adaptive schemes [50]. It is

Table 2: Average BER for all RP and BRSS for relay numbers 3 and 4 (R4).

| Relay number | BER | | | | | |
|---|---|---|---|---|---|---|
| Best = 5 (BLSTM) | $10^{-8}$ | $10^{-9}$ | $10^{-10}$ | $10^{-11}$ | $10^{-12}$ | $10^{-13}$ |
| Best = 5 (LSTM) | $10^{-7}$ | $10^{-8}$ | $10^{-9}$ | $10^{-10}$ | $10^{-11}$ | $10^{-12}$ |
| Best = 5 (GRV) | $10^{-6}$ | $10^{-7}$ | $10^{-8}$ | $10^{-9}$ | $10^{-10}$ | $10^{-11}$ |
| Best = 4 | $10^{-5}$ | $10^{-5}$ | $10^{-7}$ | $10^{-8}$ | $10^{-9}$ | $10^{-10}$ |
| All = 3 | $10^{0}$ | $10^{1}$ | $10^{-1}$ | $10^{-2}$ | $10^{-1}$ | $10^{-4}$ |
| All = 4 | $10^{-1}$ | $10^{-2}$ | $10^{-3}$ | $10^{-4}$ | $10^{-5}$ | $10^{-6}$ |
| Best = 3 | $10^{-3}$ | $10^{-4}$ | $10^{-5}$ | $10^{-6}$ | $10^{-7}$ | $10^{-8}$ |

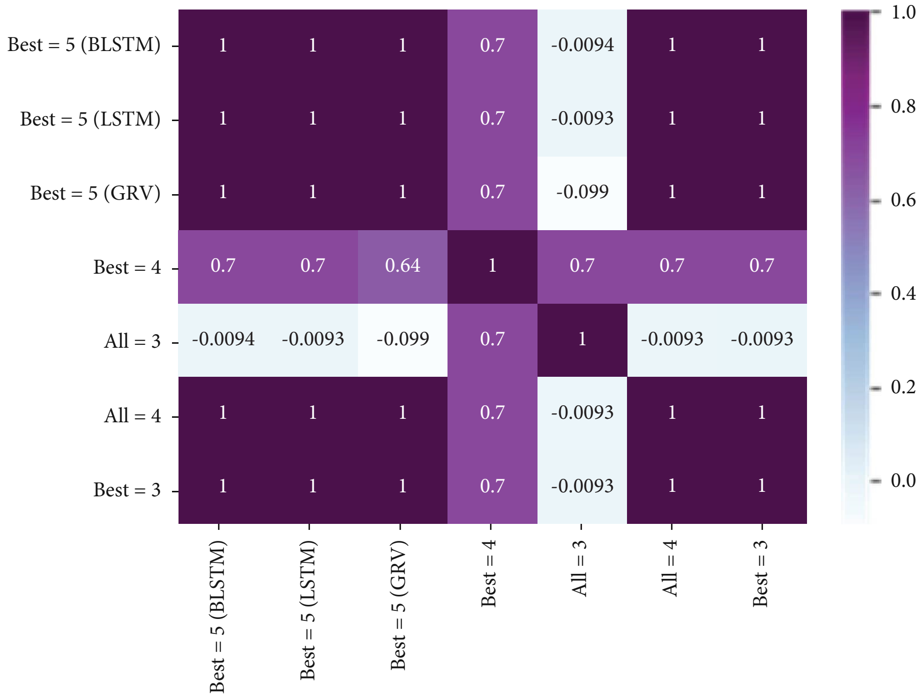


Figure 5: Heatmap co-variance relation for average BER for all RP and BRSS for relay numbers 3 and 4 (R4).

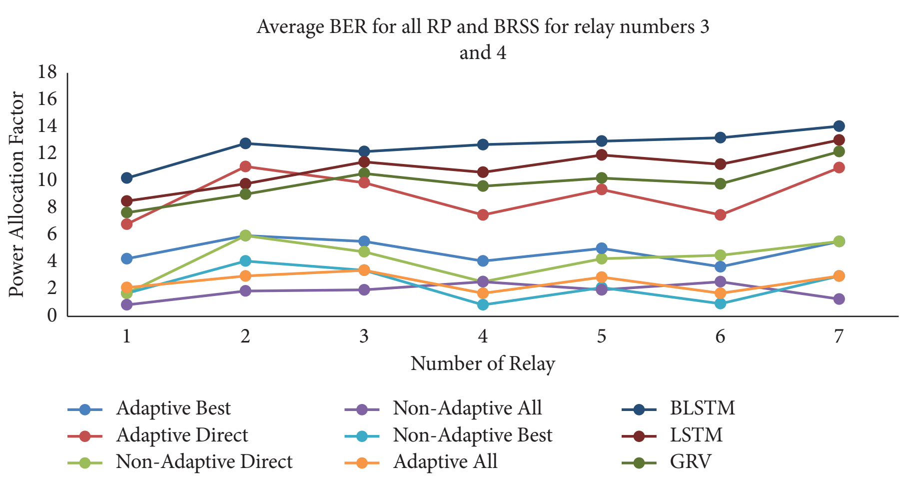


Figure 6: PA factors for different relaying schemes for varying relay numbers.

observed that the direct transmission scheme provides the greatest average PA than the other two schemes. It is also observed that BRSS outperforms the all relay participation scheme by 3 bits/s at high SNR.

Figure 7 shows the co-variance relation for spectral efficiency curves of adaptive all relay and adaptive BRS for different relay numbers. Figure 8 compares the throughput spectral efficiency performance curves of adaptive all relay

Table 3: PA factors for different relaying schemes for varying relay numbers.

| Scheme | Power allocation factor (b/J) | | | | | | |
|---|---|---|---|---|---|---|---|
| BLSTM | 12 | 15 | 14.3 | 14.5 | 15 | 15.6 | 16 |
| LSTM | 10 | 13.3 | 13.9 | 13.1 | 14.3 | 13 | 15.5 |
| GRV | 9 | 13 | 13.3 | 12 | 12 | 11 | 14.2 |
| Adaptive best | 5 | 7 | 6.5 | 5 | 6 | 4.5 | 6.5 |
| Adaptive direct | 8 | 14 | 12.5 | 9 | 11 | 9 | 13 |
| Non-adaptive direct | 2 | 7 | 6 | 3 | 5 | 5 | 6.5 |
| Non-adaptive all | 1.5 | 2 | 2 | 3 | 2.5 | 3 | 2 |
| Non-adaptive best | 2 | 3.5 | 3 | 2 | 2.5 | 2 | 3 |
| Adaptive all | 2.5 | 3 | 3 | 2.5 | 3 | 2.5 | 3 |

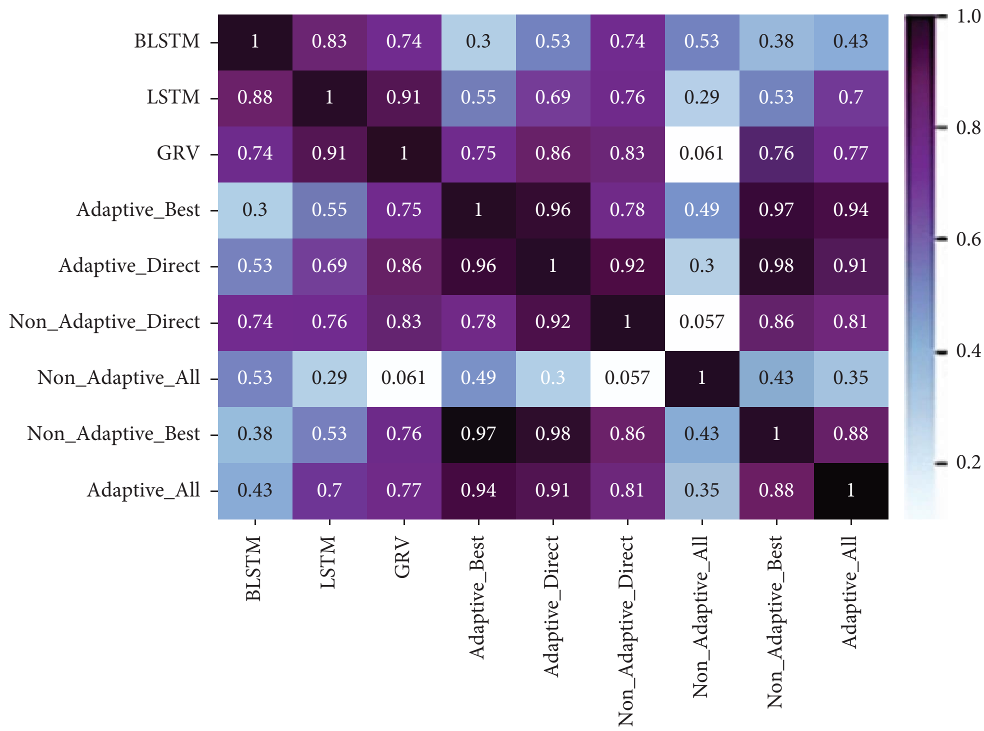


Figure 7: Heatmap co-variance relation for spectral efficiency curves of adaptive all relay and adaptive BRS for different relay numbers.

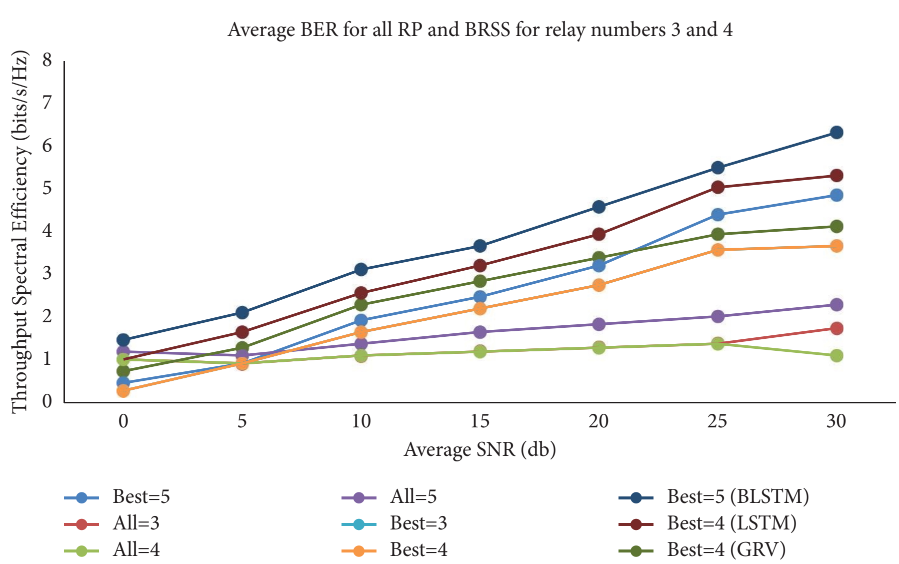


Figure 8: Throughput spectral efficiency curves of adaptive all relay and adaptive BRS for different relay numbers.

Table 4: Throughput spectral efficiency curves of adaptive all relay and adaptive BRS for different relay numbers.

| Relay number | Throughput spectral efficiency | | | | | | |
|---|---|---|---|---|---|---|---|
| Best = 5 (BLSTM) | 1.3 | 1.9 | 2.8 | 3.5 | 4.2 | 5.3 | 6 |
| Best = 5 (LSTM) | 1 | 1.6 | 2.5 | 3.3 | 3.9 | 5 | 5.3 |
| Best = 5 (GRV) | 0.9 | 1.4 | 2 | 3 | 3.6 | 4.4 | 4.6 |
| Best = 5 | 0.6 | 1 | 1.8 | 2.6 | 3.5 | 4.7 | 5.1 |
| All = 3 | 1 | 1 | 1.2 | 1.3 | 1.5 | 1.7 | 1.9 |
| All = 4 | 1 | 1 | 1.2 | 1.3 | 1.5 | 1.7 | 1.9 |
| All = 5 | 1.2 | 1.3 | 1.5 | 1.7 | 2 | 2.3 | 2.4 |
| Best = 3 | 0.5 | 1 | 1.7 | 2.5 | 3.3 | 4 | 4.4 |
| Best = 4 | 0.5 | 1 | 1.7 | 2.5 | 3.3 | 4 | 4.4 |

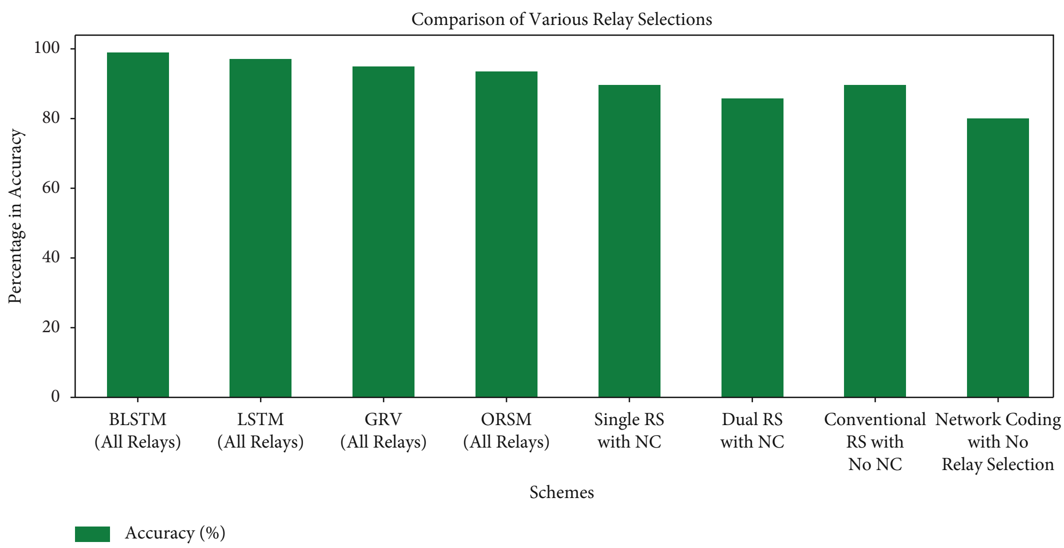


Figure 9: Comparison of various relay selections.

Table 5: Comparison of various relay selections.

| Scheme | Accuracy (%) |
|---|---|
| BLSTM (with all relays) | 98 |
| LSTM | 97 |
| GRV | 94 |
| ORSM | 93 |
| Single RS with NC (SRS-NC) | 89 |
| Dual RS with NC (DRS-NC) | 85 |
| Conventional RS with No NC (CRS-No-NC) | 88 |
| Network coding with no relay selection (NC-No-RS) | 80 |

and adaptive BRS for various relay numbers as a function of average SNR [51]. From these figures and values given in Table 4, it has been observed that adaptive BRSS outperforms the all relay scheme by 0.7 bits/s at medium SNR and about 2.5 bits/s at high SNR [52]. Figure 8 shows the relation of various relay system mechanism and BLSTM integrated relay mechanism shows the best co-relation with all the relaying schemes for spectral efficiency parameters.

The comparison of accuracy for various relay selection methods is shown in Figure 9 as well as the percentage of accuracy is given in Table 5. It has been noticed from Figure 9 that the proposed ORSM method produces the highest accuracy of about 93%. Around 4% of accuracy has been improved when compared with existing methods [53].

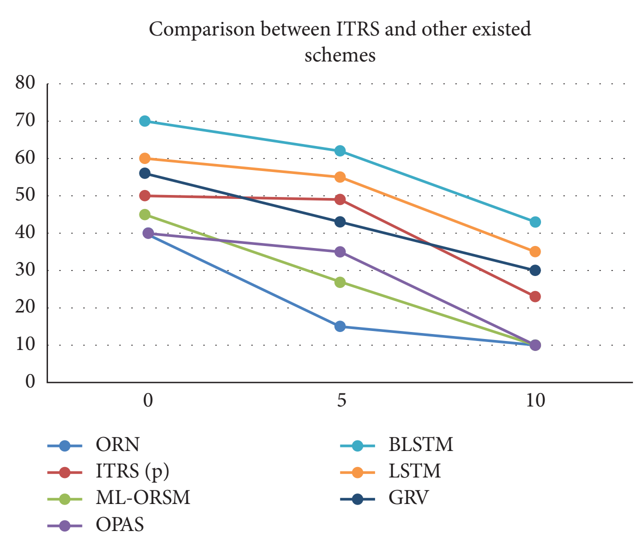


Figure 10: Comparison between ITRS and other existing schemes.

Figure 10 provides the comparison between the proposed ITRS system and other existing systems like ORN, ML-ORSM, and OPAS. The suggested ITRS scheme, with an SNR of 36 dB, is shown to give the maximum SNR and minimum BER as $10^{-6}$ when compared with the other

Table 6: Comparison between proposed and other existing techniques.

| Different relay selection schemes | BER | Average SNR(dB) |
|---|---|---|
| BLSTM | $10^{-8}$ | 38 |
| LSTM | $10^{-7}$ | 37 |
| GRV | $10^{-6}$ | 36 |
| ITRS (PS) | $10^{-6}$ | 36 |
| ORN | $10^{-5}$ | 23 |
| ML-ORSM | $10^{-5}$ to $10^{-6}$ | 32 |
| OPAS | $10^{-5}$ to $10^{-6}$ | 25 |

existing systems [54–59]. The numerical values of such comparisons are given in Table 6.

## 6. Conclusion

In recent years, CC technology has become a hotspot for testing WCNs. It will become a major component of future wireless communication systems' spectrum utilization. This system shares available channels across numerous relay nodes to boost throughput. We describe the WCNs' coordination processes as a recurrent mechanism and offer a deep learning-based transfer decision; we propose a RNN process-based relay selection. Without a model or prior data, this network is trained based on the joint receiver and transmitter outage likelihood and shared knowledge to identify the best relay from a set of relay nodes. We employ RNN to accomplish superdimensional (high-layered) processing and accelerate the rate of learning. We also use a neural network to test the communication device, determine if it can be used, how much the system can do, and how much energy the network needs. In simulations, RNN is more effective on these targets and keeps the design converged longer. We will compare our RNN-processed relay selection methods with LSTM, GRU, and BLSTM methods. Observations indicate that adaptive BRSS beats the all-relay system by 0.7 bits/s at medium SNR and by about 2.5 bits/s at high SNR. Also displayed is a comparison of the accuracy of various relay selection methods. It has been observed that the suggested ORSM method achieves an accuracy of approximately 93%, which is approximately 4% higher than existing methods.

## Nomenclature

| | |
|---|---|
| 5G: | Fifth generation |
| AES: | Advanced encryption standard |
| AF: | Amplify-and-forward |
| AI: | Artificial intelligence |
| ANN: | Artificial neural network |
| BER: | Bit error rate |
| BLSTM: | Bidirectional long short-term memory method |
| BRS-DF: | Best relay selection-based decode and forward |
| BRSS: | Best relay selection scheme |
| CC: | Cooperative communication |
| CT: | Cooperative transmission |
| CRS-No-NC: | Conventional relay selection with no network coding |
| CSI: | Channel state information |
| DSSS: | Direct sequence spread spectrum |
| DF: | Decode-and-forward |
| DRS-NC: | Dual relay selection with network coding |
| DSTC: | Distributive space time coding |
| DT: | Direct transmission |
| DL: | Deep learning |
| ED: | Energy detection |
| FC: | Fully connected |
| FHSS: | Frequency hop spread spectrum |
| FD-AF-RN: | Full duplex amplify-and-forward relay networks |
| GRU: | Gated recurrent units |
| IO: | Input output |
| ITRS: | Interference thwarting relay selection |
| KPI: | Key performance indicator |
| LAN: | Local area network |
| LSTM: | Long short-term memory |
| LTE: | Long term evolution |
| MCS: | Modulation and coding scheme |
| ML-ORSM: | Machine learning-optimal relay selection method |
| MU: | Mobile user |
| NC: | Network coding |
| NC-No-RS: | Network coding with no relay selection |
| OPAS: | Optimal power allocation scheme |
| ORN: | Optimal relay node |
| ORSM: | Optimal relay selection method |
| PA: | Power allocation |
| PDF: | Probability distribution function |
| QoS: | Quality of service |
| RP-DF: | Relay participate decode and forward |
| RS: | Relay selection |
| RNN: | Recurrent neural network |
| SER: | Symbol error rate |
| SNR: | Signal to noise ratio |
| SRS-NC: | Single relay selection with network coding |
| SVM: | Support vector machine |
| V-MIMO: | Virtual-multiple input multiple output |
| VR: | Virtual reality |
| WAP2: | Wi-fi protected access 2 |
| WEP: | Wire equivalent privacy |
| WN: | Wireless network |
| WCNs: | Wireless communication networks. |

## Data Availability

The data are used to support the findings of this study are included within the article.

## Conflicts of Interest

The authors declare that they have no conflicts of interest.

## References


[1] B. Sirkeci-Mergen and S. Moballegh, "Broadcasting in dense linear networks: to cooperate or not to cooperate?" *Ad Hoc Networks*, vol. 83, pp. 182–197, 2019.

[2] I. Dey, P. Salvo Rossi, M. M. Butt, and N. Marchetti, "Virtual MIMO wireless sensor networks: propagation measurements and fusion performance," *IEEE Transactions on Antennas and Propagation*, vol. 67, no. 8, pp. 5555–5568, 2019.

[3] S. Bastanirad, S. Shahbazpanahi, R. Rahimi, and A. Grami, "On total transmission power minimization approach to decentralized beamforming in single-carrier asynchronous bidirectional relay-assisted communication networks," *IEEE Access*, vol. 7, pp. 30966–30979, 2019.

[4] D.&T. Mishra, A. Trotta, E. Traversi, M. D. Felice, and E. Natalizio, "Cooperative Cellular UAV-to-Everything (C-U2X) communication based on 5G sidelink for UAV swarms," *Computer Communications*, vol. 192, pp. 173–184, 2022.

[5] M. S Al-kahtani and S. Mohammed, "A review of relay assignment problem in the cooperative wireless sensor networks," *Electronics*, vol. 9, no. 3, p. 443, 2020.

[6] Y. H. Al-Badarneh, C. N. Georghiades, and M. S. Alouini, "Asymptotic performance analysis of generalized user selection for interference-limited multiuser secondary networks," *IEEE Transactions on Cognitive Communications and Networking*, vol. 5, no. 1, pp. 82–92, 2019.

[7] P. Fabian and R. Abderrezak, "Dynamic selection of relays based on classification of mobilityprofile in a highly mobile context," in *Proceedings of the ICC 2020 - 2020 IEEE International Conference on Communications(ICC)*, pp. 1–6, Dublin, Ireland, June 2020.

[8] Q. Zhu, Z. Chen, and X. He, "Resource allocation for relay-based OFDMA power line communication system," *Electronics*, vol. 8, no. 2, p. 125, 2019.

[9] M. B. Laghari, H. Shahwani, S. A. Shah et al., "Towards enabling multihop wireless local area networks for disaster communications," *Wireless Communications and Mobile Computing*, vol. 2021, Article ID 5540480, 14 pages, 2021.

[10] N. N. Dao, M. Park, J. Kim, J. Paek, and S. Cho, "Resource-aware relay selection for inter-cell interference avoidance in 5G heterogeneous network for Internet of Things systems," *Future Generation Computer Systems*, vol. 93, pp. 877–887, 2019.

[11] A. Mchergui, T. Moulahi, and S. Nasri, "Relay selection based on deep learning for broadcasting in vanet," in *Proceedings of the 2019 15 th International Wireless Communications & Mobile Computing Conference (IWCMC)*, pp. 865–870, IEEE, Tangier, Morocco, 2019, June.

[12] N. Heydarishahreza, S. Ebadollahi, R. Vahidnia, and F. J. Dian, "Wireless sensor networks fundamentals: a review," in *Proceedings of the 11th IEEE Annual Information Technology, Electronics and Mobile Communication Conference (IEMCON)*, pp. 0001–0007, Vancouver, BC, Canada, November 2020.

[13] J.-J. Bao, Q. Mai, and J. F. Tu, "Study of cooperative strategy based on space–time labeling diversity in indoor visible light communication systems," *Symmetry*, vol. 12, no. 5, p. 702, 2020.

[14] A. E. Gamal, A. Gohari, and C. Nair, "Achievable Rates for the Relay Channel with Orthogonal Receiver Components," in *Proceedings of the 2021 IEEE Information Theory Workshop (ITW)*, pp. 1–6, Kanazawa, Japan, October 2021.

[15] S. Chen, J. Zhang, Y. Lin et al., "Cell-free massive mimo: a new next-generation paradigm," *IEEE Access*, vol. 7, pp. 99878–99888, 2019.

[16] Z. Wang, Z. Peng, Y. Pei, and H. Wang, "Performance analysis of cooperative NOMA systems with incremental relaying," *Wireless Communications and Mobile Computing*, vol. 2020, Article ID 4915638, 15 pages, 2020.

[17] P. T. Hiep and T. M. Hoang, "Non-orthogonal multiple access and beamforming for relay network with RF energy harvesting," *ICT Express*, vol. 6, no. 1, pp. 11–15, 2020.

[18] H. Hai, C. Li, J. Li, Y. Peng, J. Hou, and X. Q. Jiang, "Space-time block coded cooperative MIMO systems," *Sensors*, vol. 21, no. 1, p. 109, 2020.

[19] S. Abdallah, A. I. Salameh, and M. Saad, "Spectrum efficient joint frequency offset and channel estimation for time-asynchronous amplify-and forward two-way relay networks," *IEEE Access*, vol. 7, pp. 71972–71985, 2019.

[20] C.-C. Chen and M.-L. Ku, "Carrier frequency offset estimation bound for OFDM-based single relay networks with multipath receptions," *IEEE Access*, vol. 7, pp. 63900–63912, 2019.

[21] H. M. Al-Obiedollah, K. Cumanan, J. Thiyagalingam et al., "Spectral-energy efficiency trade-off-based beamforming design for MISO non-orthogonal multiple access systems," *IEEE Transactions on Wireless Communications*, vol. 19, no. 10, pp. 6593–6606, 2020.

[22] R. Kumar and A. Hossain, "Survey on Half- and Full-Duplex Relay Based Cooperative Communications and its Potential Challenges and Open Issues Using Markov Chains," *IET Communications*, vol. 13, pp. 1537–1550, 2019.

[23] J. Y. Lai, W.-H. Wu, and Y. T. Su, "Resource allocation and node placement in multi-hop heterogeneous integrated-access-and-backhaul networks," *IEEE Access*, vol. 8, pp. 122937–122958, 2020.

[24] Z. Wang, H. Hu, B. Jia, and T. Xu, "A windowing-based joint user pairing and resource allocationalgorithm for V-MIMO systems," *Computer Communications*, vol. 144, pp. 1–7, 2019.

[25] D. Liu, J. Wang, Y. Xu, Y. Xu, Y. Yang, and Q. Wu, "Opportunistic mobility utilization in flying ad-hoc networks: a dynamic matching approach," *IEEE Communications Letters*, vol. 23, no. 4, pp. 728–731, 2019.

[26] K. Kim, J. Kim, and Y. Shin, "Parallelised relaying protocol with opportunistic priority assignment for enhanced spectral efficiency in cross-relay interference," *IET Communications*, vol. 13, no. 7, pp. 934–938, 2019.

[27] W. Jiang and H. D. Schotten, "Deep learning for fading channel prediction," *IEEE Open Journal of the Communications Society*, vol. 1, pp. 320–332, 2020.

[28] H. D. Schotten, W. Jiang, H. D. Schotten, and H. D. Schotten, "Neural network-based fading channel prediction: a comprehensive overview," *IEEE Access*, vol. 7, pp. 118112–118124, 2019.

[29] W. Jiang and H. D. Schotten, "A simple cooperative diversity method based on deep-learning-aided relay selection," *IEEE Transactions on Vehicular Technology*, vol. 70, no. 5, pp. 4485–4500, 2021.

[30] M. M. Akho-Zahieh and N. Abdellatif, "Performance analysis of MIMO wavelet packet multicarrier multicode CDMA system with antenna selection," *Advances in Electrical and Electronic Engineering*, vol. 17, no. 4, 2019.

[31] S. W. H. Shah, M. M. U. Rahman, A. N. Mian, O. A. Dobre, and J. Crowcroft, "Effective capacity analysis of HARQ-enabled D2D communication in multi-tier cellular networks,"

*IEEE Transactions on Vehicular Technology*, vol. 70, no. 9, pp. 9144–9159, 2021.
[32] M. G. Ri, Y. S. Han, and J. Pak, "A distributed energy-efficient opportunistic routing accompanied by timeslot allocation in wireless sensor networks," *International Journal of Distributed Sensor Networks*, vol. 18, no. 5, p. 155014772110499, 2022.
[33] T. Charalambous, S. M. Kim, N. Nomikos, M. Bengtsson, and M. Johansson, "Relay-pair selection in buffer-aided successive opportunistic relaying using a multi-antenna source," *Ad Hoc Networks*, vol. 84, pp. 29–41, 2019.
[34] A. Subhash and S. Kalyani, "Cooperative relaying in a SWIPT network: asymptotic analysis using extreme value theory for non-identically distributed RVs," *IEEE Transactions on Communications*, vol. 69, no. 7, pp. 4360–4372, 2021.
[35] C. Zhang, H. Lin, Y. Huang, and L. Yang, "Performance of integrated satellite-terrestrial relay network with relay selection and outdated CSI," *IEEE Access*, vol. 8, pp. 169652–169662, 2020.
[36] Y. Zhang, Y. Su, X. Shen et al., "Reinforcement learning based relay selection for underwater AcousticCooperative networks," *Remote Sensing*, vol. 14, no. 6, p. 1417, 2022.
[37] Z. Bhutto and W. Yoon, "Dual-hop cooperative relaying with BeamformingUnder adaptive transmission in $\kappa$–$\mu$ shadowed fading environments," *Electronics*, vol. 8, no. 6, p. 658, 2019.
[38] E. Fidan and O. Kucur, "Performance of cooperative full-duplex AF relay networks with generalised relay selection," *IET Communications*, vol. 14, no. 5, pp. 800–810, 2020.
[39] Volkan, "Leakage Rate-Based Untrustworthy Relay Selection with Imperfect Channel State Information," *The Outage and Security Trade-Off Analysis*, vol. 13, no. 13, pp. 1902–1915, 2019.
[40] R. Mukherjee and K. S. Patnaik, "A survey on different approaches for software test case prioritization," *Journal of King Saud University - Computer and Information Sciences*, vol. 33, no. 9, pp. 1041–1054, 2021.
[41] W. Jiang, M. Strufe, and H. Dieter Schotten, "Long-range MIMO channel prediction using recurrent neural networks," in *Proceedings of the 2020 IEEE 17th Annual Consumer Communications & Networking Conference (CCNC)*, pp. 1–6, Las Vegas, NV, USA, January 2020.
[42] K Vaibhav, C. Barry, and F. Mark, "Performance Analysis of NOMA with Generalised Selection Combining Receivers," *Flanagan*, vol. 55, no. 25, pp. 1364–1367, 2019.
[43] S. Jain and B. Ranjan, "QVP-Based Relay Selection to Improve Secrecy for Rateless-Codes in Delay," *Constrained Systems*, vol. 13, no. 1, pp. 26–35, 2019.
[44] F. Mezghani and N. Mitton, "Opportunistic multi-technology cooperative scheme and UAV relaying for network disaster recovery," *Information*, vol. 11, no. 1, p. 37, 2020.
[45] E. Eyceyurt, Y. Egi, and J. Zec, "Machine-learning-based UplinkThroughput prediction from PhysicalLayer measurements," *Electronics*, vol. 11, no. 8, p. 1227, 2022.
[46] C. Lv, J.-C. Lin, and Z. Yang, "Channel prediction for millimeter wave MIMO-OFDM communications in rapidly time-varying frequency-selective fading channels," *IEEE Access*, vol. 7, pp. 15183–15195, 2019.
[47] Z. Wang, W. Xie, Y. Zou, and Q. Wan, "DOA estimation using single or dual reception channels based on cyclostationarity," *IEEE Access*, vol. 7, pp. 54787–54795, 2019.
[48] A. M. Aldosary, S. A. Aldossari, K.-C. Chen, E. M. Mohamed, and A. Al-Saman, "Predictive WirelessChannel modeling of MmWaveBands using machine learning," *Electronics*, vol. 10, no. 24, p. 3114, 2021.
[49] Y. Gao and L. Wu, "Efficiently mastering the game of NoGo with deep reinforcement learning supported by domain knowledge," *Electronics*, vol. 10, no. 13, p. 1533, 2021.
[50] H. B. Hewamalage and K. Christoph&Bandara, "Recurrent Neural Networks for Time Series Forecasting: Current Status and Future Directions," 2019, https://arxiv.org/abs/1909.00590.
[51] W. Jiang and H. D. Schotten, "Deep learning for fading channel prediction," *IEEE Open Journal of the Communications Society*, vol. 1, pp. 320–332, 2020.
[52] W. Jiang, H. DieterSchotten, and J. Y. Xiang, *Neuralnetwork–Basedwirelesschannelprediction.Machine Learning for Future Wireless Communications*, pp. 303–325, Wiley, New Jersey, U.S.A, 2020.
[53] C. Eom and C. Lee, "Hybrid neural network-based fading channel prediction for link adaptation," *IEEE Access*, vol. 9, pp. 117257–117266, 2021.
[54] R. Staudemeyer and E. Morris, "Understanding lstm -- a tutorial into long short-term memory recurrent neural networks," 2019, https://arxiv.org/abs/1909.09586.
[55] W. Jiang and H. D. Schotten, "Recurrent Neural Networks with Long Short-Term Memory for Fading Channel Prediction," in *Proceedings of the 2020 IEEE 91st Vehicular Technology Conference (VTC2020-Spring)*, pp. 1–5, Antwerp, Belgium, May 2020.
[56] H. Okut, *Deep learning for subtyping and prediction of diseases: long-short term memory Deep Learning Applications*, P. Mazzeo and P. Spagnolo, Eds., IntechOpen, London, U.K, 2021.
[57] H. O. Hirose and G. Tomoaki&Gui, "Deep Learning-Based Channel Estimation for Massive MIMO Systems with Pilot Contamination," *IEEE Open Journal of Vehicular Technology*, vol. 2, pp. 67–77, 2020.
[58] J.-C. Lin and H. V. Poor, "Optimum combiner for spatially correlated nakagami-m fading channels," *IEEE Transactions on Wireless Communications*, vol. 20, no. 2, pp. 771–784, 2021.
[59] I. S. Gradshteyn, I. M. Ryzhik, and D. F. Hays, "Table of integrals, series, and products," *Journal of Lubrication Technology*, vol. 98, no. 3, p. 479, 1976.